RAMReS Sciences des Structures et de la Matière Vol. 7, N°2 (2023) 116 - 131
http://publication.lecames.org/index.php/mat ISSN: 2630-1180

Characterization of link for free-Space terrestrial optical communications in Côte d'Ivoire

Douatia Koné[1,2,*], Niangoran Medard Mene[1], Aladji Kamagaté[1,3]

[1]*Mathematics-Physics-Chemistry Department, Université Péléforo Gon Coulibaly, Korhogo, Côte d'Ivoire*
[2]*Research and Technological Innovation Department, Ecole Supérieure Africaine des Technologies de l'Information et de la Communication, Abidjan, Côte d'Ivoire*
[3]*Digital and Mathematics Department, Agence National de Recherche, Paris, France*

Received: 29 September 2023 / Received in revised form: 27 November 2023 / Accepted: 4 December 2023

***Abstract*:**
We investigate the availability of a terrestrial free-space optical communication system under different levels of atmospheric turbulence in Côte d'Ivoire. Thanks to the Gamma-gamma distribution, nature of the turbulence and its effects on the optical link have been explored in five sites, which represent different atmospheric and meteorological conditions in Côte d'Ivoire d'Ivoire (Abidjan, Bouaké, Korhogo, Man, and Bondoukou). The nature of atmospheric turbulence in our environments was described using an assessment of the refractive index structure parameter. An analysis of error probability was conducted across various environments. It was discovered that the deterioration of the signal caused by atmospheric conditions in the typical circumstances of Côte d'Ivoire is not particularly substantial. Additionally, the height of the environment significantly impacts the natureof atmospheric turbulence.

***Keywords*:** Error Probability; FSO; Gamma-gamma distribution; K distribution; Log-Normal distribution; SNR; Côte d'Ivoire.

1 Introduction

Augmented reality, streaming, ultra-high definition television, connected objects, and computer applications necessitate exceptionally high bandwidth levels for proficient operation [1]. These systems, combined with the rise of social media, which have done much to change people's habits of interaction, and the development of military UAV (unmanned aerial vehicle) guidance systems, make it all the more important to disseminate information via high-speed interconnection systems [1].

*Corresponding author:
Email address: douatiaben@gmail.com (*D. Koné*)

To meet these needs, various communication systems have been developed, such as radio frequency communication systems (microwave, GSM, LTE, 4G), sound communication systems, and systems based on optical technologies such as fibre optics, visible communication systems (VLC), and free space communication systems (FSO) [2]. Compared with communication techniques based on commonly used radio frequency technologies, FSO systems offer better performance in terms of throughput, deployment costs and intrinsic security [3]. This technology is based on the use of laser beams to transmit information in the form of light through the atmospheric channel at data rates of up to 100 Gbps [4]. The wavelength generally used for commercial systems is 1550 nm for telecommunications applications [1]. The use of the atmosphere as a propagation channel by FSO technology means that its performance depends on the atmospheric conditions of its operating environment [3]. In order to guarantee the proper functioning of this technology within a certain environment, it is crucial to have an accurate understanding of the nature of the atmospheric turbulence present in that environment, as well as its effects on the accessibility of said systems [3, 4]. It is in this context that in 2019 a study by Shahiduzzaman *et al.* [5] to characterize the atmospheric channel in Bangladesh showed that the atmospheric scattering effect does not hinder the performance of the short-range FSO link, whereas the atmospheric turbulence effect can strongly influence the deployment of FSO technology in Bangladesh. A second study carried out at Owerri in Nigeria by Ayo-Akanbi *et al.* [6] revealed that the outage probability of FSO systems in subtropical atmospheric conditions in West Africa could be of the order of 10^{-2}.

In the present study, we examine the atmospheric channel of Côte d'Ivoire, focusing on the regions of Korhogo, Man, Bouaké, Bondoukou, and Abidjan. We then characterize the nature of its turbulence and analyse its impact on the availability of the FSO link in each of the selected city. Atmospheric scintillation and the probability of error are also studied. Section 2 presents an overview of FSO systems, while section 3 presents the results combined with discussion and analysis. Section 4 concludes the paper.

2 Overview of FSO system

Free-space optical communication is based on line-of-sight (LOS) between communication points [1]. It uses a laser source to transmit data in the infrared and visible ranges. The small size of the beams means that the link is intrinsically safe and relatively robust. Free-space optical communication is theoretically possible provided there is line-of-sight between the source and the destination. The FSO system has three parts: transmission, propagation channel and reception [1, 7]. The process of operation of optical systems in free space is described in Figure 1 [7]. In this study, we are particularly interested in the propagation channel, which is the environment in which the light beam propagates. The atmospheric environment has complex properties that can vary from moment to moment, affecting the characteristics of the light beam propagating through it. FSO links are subject to several limitations imposed by the atmospheric propagation environment. These limitations can result in attenuation or extinction of the optical signal during propagation, leading to a reduction in the range between the transmitter and receiver [1].

2.1 Atmospheric channel modelling

There are several empirical models for characterizing atmospheric turbulence. In this section we present the three most commonly used models families for characterizing the atmospheric channel, namely the

normal model, the exponential model and the gamma-gamma model [1,8].

2.1.1 Log-normal model

The normal distribution family is one of the first statistical probability families developed to describe natural phenomena that evolve randomly [8]. In the FSO context, the most widely used normal distribution model is the log-normal model [9]. The probability density function (PDF) of this model derives directly from Rytov's first approximation [8], and adapts well to low turbulence environments [7]. Consequently, in these environments, it has been the model most often used to calculate the fading statistics associated with a fading communication channel. However, more recent studies of the Log-normal PDF suggest that it can be used to predict fading probabilities in moderately fluctuating regimes [8,9]. The Log-Normal model assumes that the random variable defined by the logarithm of the irradiance $ln(I)$ follows a normal distribution due to channel turbulence [8]. The probability density $\rho_I I(I)$ for the Log-Normal model is given by equation (1) [7,8],

$$\rho_I(I) = \frac{1}{I\sigma\sqrt{2\pi}} exp\left(-\frac{(ln(I)+\frac{\sigma^2}{2})}{2\sigma^2}\right) \quad (1)$$

Where σ^2 is the variance of the random variable $ln(I)$ which depends on the characteristics of the channel. Equation (2) can be used to determine its values [8],

$$\sigma^2 = exp\left(\frac{0.49\delta^2}{(1+0.18d^2+0.56\delta^{12/5})^{7/6}} + \dots \frac{0.51\delta^2}{(1+0.9d^2+0.62d^2\delta^{12/5})^{5/6}}\right) \quad (2)$$

with $d = (kD^2/4L)^{1/2}$ & $k = 2\pi/\lambda$ the wave number. D is the diameter of the receiver aperture, and L is the propagation distance. The Rytov variance is expressed as $\delta = 1.23C_n^2 k^{7/6} L^{11/6}$, where C_n^2 is the structural parameter of the refractive index of the atmosphere [10].

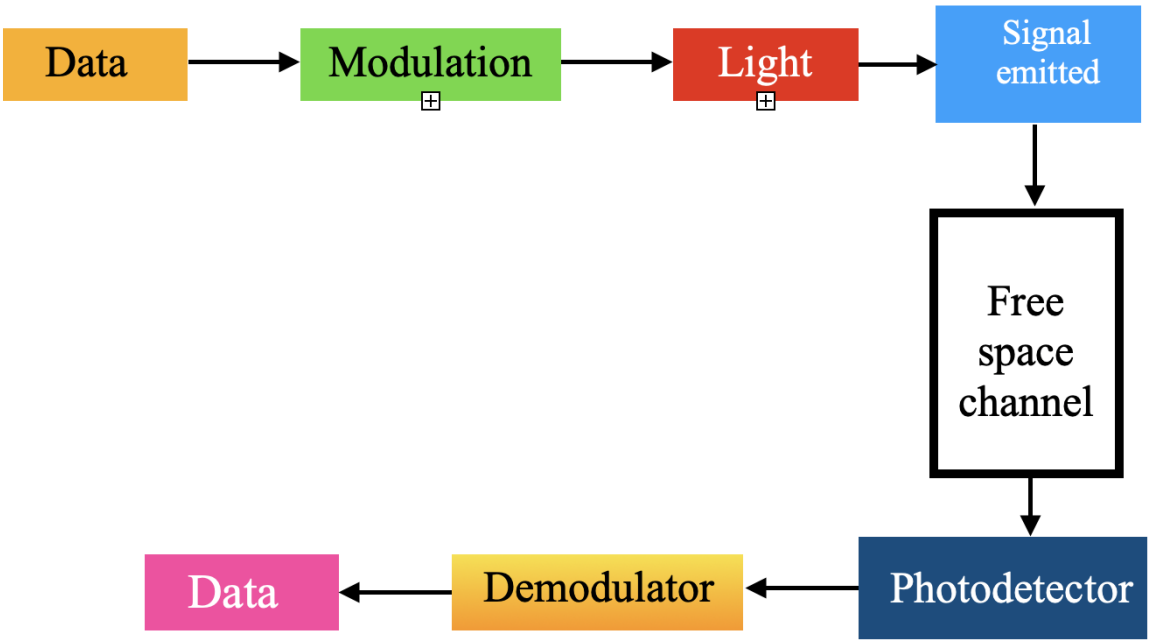

Fig. 1. The process of operation of optical systems in free space.

2.1.2 K-distribution model

One of the first models to be best adapted to characterize the regimes of strong turbulence is the K distribution [7, 11]. In fact, the general family of K distributions can be used to accurately predict irradiance statistics in several types of experiment involving radiation attenuated by highly turbulent media [11]. This distribution is derived from a modulation process of a negative exponential distribution and a gamma distribution. This can be seen in equation (3) [7, 12].

$$\rho(I) = \frac{2\alpha}{\Gamma(\alpha)}(\alpha I)^{(\alpha-1)/2} K_{\alpha-1}(2\sqrt{\alpha I}) \quad I\rangle 0 \tag{3}$$

where $K_p(x)$ is a modified Bessel function of the second kind. This is why the PDF is known as the K distribution. Also, when $\alpha \to \infty$, the K distribution tends towards a negative exponential distribution (i.e. the gamma distribution approaches a Dirac delta function) [13].

2.1.3 Gamma-gamma model

In this model, radiation is modelled as the result of two statistically independent processes: one for small-scale effects and the other for the large-scale effects modelled by each gamma [1] distribution. This characteristic gives it the ability to accurately characterize environments with low, moderate and high turbulence [14]. Another important feature of this model is that its parameters depend directly on the atmospheric conditions of the environment. [1, 14]. For this study we will use the Gamma-gamma distribution model. Widely used by researchers, this model, unlike other models, accurately models weak turbulence, moderate turbulence and strong turbulence. It will therefore enable us to accurately describe the nature of turbulence in our environment. The PDF of irradiance for this model is given by equation (4) [1, 8].

$$\begin{aligned} &\rho(I) = \frac{2(\alpha\beta)^{(\alpha+\beta)/2}}{\Gamma(\alpha)\Gamma(\beta)} \times \dots \\ &I^{\frac{\alpha+\beta}{2}-1} K_{\alpha-\beta}(2\sqrt{\alpha\beta I}) \qquad I\rangle 0 \end{aligned} \tag{4}$$

where $K_p(x)$ is the modified Bessel function of the second kind, $\Gamma(x)$ is the Euler Gamma function, α is the effective number of small-scale turbulences and β the effective number of large-scale turbulences. The values of α and β are given by equations (5) and (6) [8].

$$\alpha = [exp(\frac{0.49\sigma^2}{1 + 1,11\sigma^{12/5}})^{7/6} - 1]^{-1} \tag{5}$$

and

$$\beta = [exp(\frac{0.51\sigma^2}{1 + 0.69\sigma^{12/5}})^{5/6} - 1]^{-1} \tag{6}$$

with σ^2 the temperature variation between the ground and the atmosphere, given by equation 7 [1, 8].

$$\sigma^2 = 1,23 C_n^2 k^{7/6} L_p^{11/6} \tag{7}$$

σ^2 is called the Rytov variance (or scintillation index). We have Lp the path length, k the wave number ($k = \frac{2\pi}{\lambda}$) and C_n^2 the refractive index structure parameter.
In this study we use the Gamma-gamma distribution, unlike other distributions (log-normal distribution and K distribution) whose performances are optimal only in cases of weak turbulence for normal distributions and for cases of strong turbulence for distributions exponential. The Gamma-gamma distribution presents the best performances for the characterization of turbulence in weak, medium, and strong turbulence regimes. This model helps to describe all king of environment under turbulence [1].

2.2 Error Probability

In the context of communications, the probability of error generally refers to the likelihood that a transmission signal will be misinterpreted or corrupted during its transmission from one point to another. This can occur due to a variety of factors, such as noise, attenuation, interference, etc. In digital communication systems, the probability of error is often used to assess the quality

of data transmission. The intensity modulation format OOK (On Off Keying), is a modulation format that allows the signal to have only two states, a zero state (0) and a positive state (1). For this modulation format, and signal distributed according to an equiprobable probability law, the value of the PB is given by equations (8) and (9) [7,9].

$$Pe = P(e, off) + P(e, on) \tag{8}$$

with $P(e, off) = P(off)P(e|off)$ and $P(e, on) = P(on)P(e|on)$. So probability of error becomes,

$$\begin{array}{l} Pe = P(off)P(e|off) + \ldots \\ P(on)P(e|on) \end{array} \tag{9}$$

with $P(off)$ and $P(on)$ the probabilities of sending "0" and "1" respectively, $P(|off)$ the probability of conditional error knowing that it is an off (0) that has been sent, and $P(e|on)$ the probability of conditional error knowing that it is an on (1) that has been sent. The values of $P(e|on)$ and $P(e|off)$ for the irradiance I are expressed from the equation (10) [15].

$$\begin{array}{l} p(e, I) = P(e|off) = P(e|on) = \ldots \\ erfc\left(\frac{\mu I}{\sqrt{2N_0}}\right) \end{array} \tag{10}$$

with μ responsivity of photodetector, N_0 noise power spectral density, and $erfc(.)$ the Gaussian error function given by equation (11) [1].

$$erfc(x) = \frac{2}{\sqrt{\pi}} = \int_0^x exp(-t^2)\,\mathrm{d}t \tag{11}$$

The signal being distributed according to an equiprobable probability law, we have $P(on) = P(off) = \frac{1}{2}$. From equation (11), we obtain equation 12 which establishes a relation between the probability of error depending on atmospheric parameters [7,8].

$$\begin{array}{l} Pe = p(e, I) = erfc\left(\frac{\mu I}{\sqrt{2N_0}}\right) \\ \rho_{Pe} = \int_0^\infty P(e|I)\rho_I(I)\,\mathrm{d}I \\ \rho_{Pe} = \int_0^\infty erfc\left(\frac{\mu I}{\sqrt{2N}}\right)\rho_I(I)\,\mathrm{d}I \\ \rho_{Pe} = \int_0^\infty erfc\left(\sqrt{\frac{\gamma}{2}}\right)\rho_I(I)\,\mathrm{d}I \end{array} \tag{12}$$

3 Results and discussion

3.1 Results

3.1.1 Presentation of test environment

Our simulations will be performed for five distinct environments, namely Korhogo, Bouaké, Abidjan, Man, and Bondoukou. This will allow us to know which environment presents the best properties for the deployment of an FSO system. For the numerical simulations, meteorological data for each of these environments were retrieved from "historique-meteo" site [16]. Figure 2 represents the different vegetations and climates of Côte d'Ivoire by region.

Korhogo located in the north of Côte d'Ivoire in West Africa, is generally characterized as a tropical savannah climate, also known as a dry tropical climate or Sudanian savannah climate. This city is located 380 m above sea level, Korhogo generally has two distinct seasons: a rainy season (wet season) and a dry season (dry season). Temperatures in Korhogo vary considerably between the seasons. Maximum temperatures can reach high values during the dry season, while the rainy season is generally cooler. Nights can be relatively cool during the dry season [17].

Bouaké is a town in Côte d'Ivoire, in West Africa. It is in the central part of the country. This city is located 312 m above sea level. Bouaké's climate is generally classified as tropical savannah, also known as dry tropical or Sudanian savannah. Bouaké generally has two distinct seasons: a rainy season (wet season) and a dry season (dry season). These seasons are marked by significant variations [17].

Abidjan is the largest city in Côte d'Ivoire and is located on the country's southern coast, on the shores of the Gulf of Guinea.

Situated 18 m above sea level, the city enjoys an equatorial climate, specifically a tropical equatorial climate, characterized by warm temperatures throughout the year and abundant rainfall [17].

Man is located in the west of Côte d'Ivoire, in the Tonkpi region. Its climate is classified as tropical equatorial. Man has a prolonged rainy season, generally from May to October. During this period, the city receives abundant rainfall, with frequent showers. The wettest months are generally June, July and August. Man is 329 m above sea level [17].

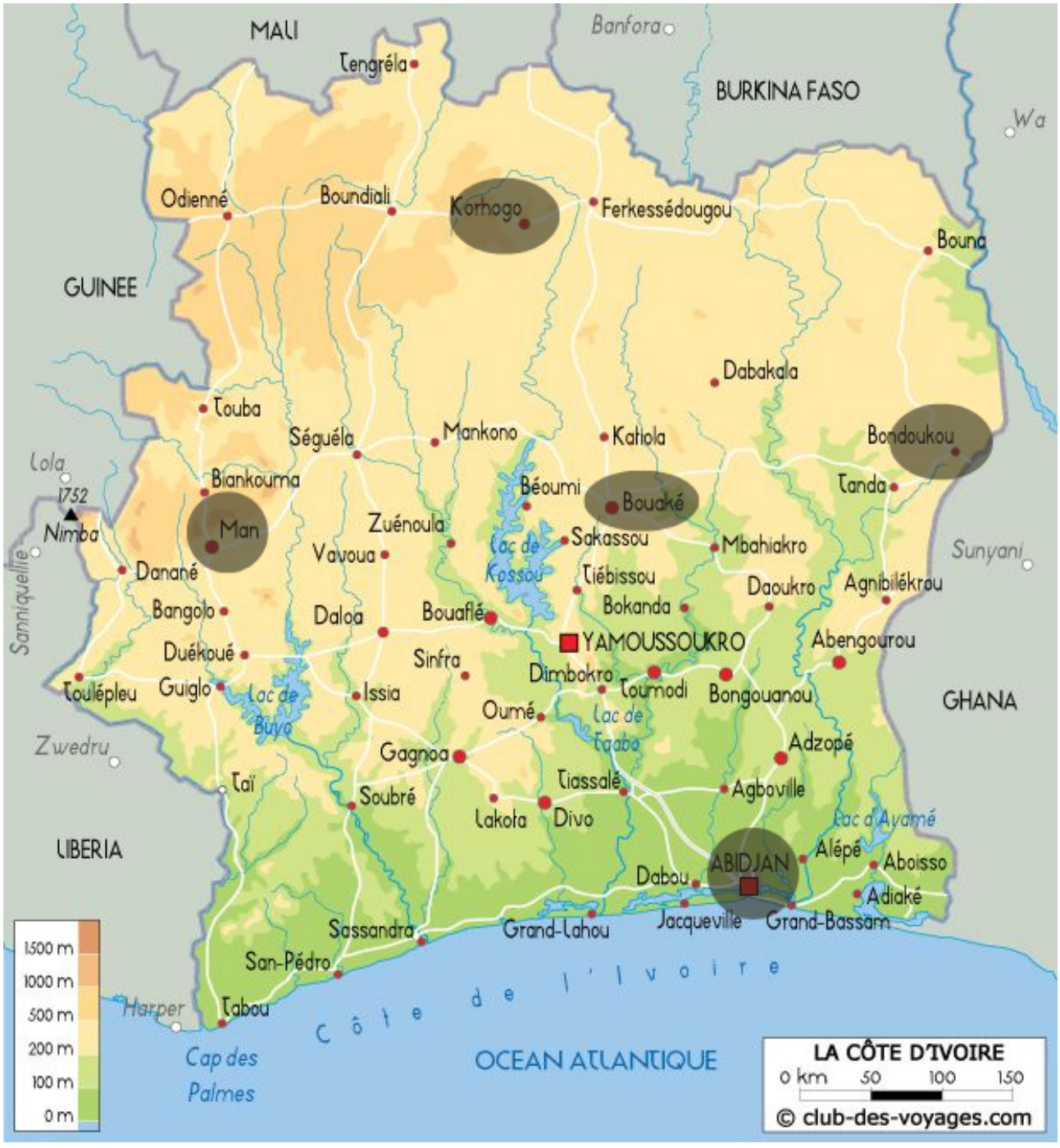

Fig. 2. Map of Côte d'Ivoire showing the studied towns.

Bondoukou is a town in the east of Côte d'Ivoire, in West Africa. Its climate is classified as tropical equatorial, similar to that of other regions close to the equator. Bondoukou experiences high temperatures throughout the year due to its position close to the equator. Average monthly temperatures vary little, with average highs generally between 30°C and 32°C. Bondoukou is 343 m above sea level [17].

3.1.2 Analysis of the distribution of atmospheric factors

Atmospheric turbulence is particularly dependent on meteorological conditions, notably visibility, precipitation and wind speed [8, 18]. These different factors make it possible to analyse the distribution of atmospheric scintillation cells, which make a major contribution to the degradation of the FSO link. Consequently, it is essential for the establishment of an FSO link to know their distribution in the propagation channel. To this end, five cities representing the different weather profiles of Côte d'Ivoire, namely Abidjan, Bouaké, Bondoukou, Man, and Korhogo, were selected and considered for the study. Visibility, wind speed and precipitation data from January 2018 to December 2022 were collected from the "weather history" platform [17]. The visibility data were used to determine the scattering effect of Mie. Some regions of Côte d'Ivoire are subject not only to heavy rainfall every year during the monsoon season, but also to light rainfall throughout the year [19]. Rainfall data can be used to describe the levels of non-selective atmospheric diffusion experienced by an FSO link. But to calculate the nature of atmospheric turbulence, only wind speed data from January 2018 to December 2022 are considered.

- **Diffusion coefficient due to mie and rain**

Visibility and precipitation data are used to determine the overall scattering coefficient. For the analysis of visibility and precipitation data, monthly data from January 2018 to December 2022 were consulted, and the maximum, minimum and average visibility and precipitation rates were calculated to analyze the scattering experienced in clear weather and in the worst conditions for our different cities. First, let's consider the effect of Mie scattering. Visibility is the parameter that directly contributes to Mie scattering, which is selective scattering. its expression is given by equation (13) [5, 8],

$$\beta_{brouillard} = \frac{3.91}{V}\left(\frac{\lambda}{\lambda_0}\right)^{-p} \qquad (13)$$

Where V (km) represents the viewing distance, λ (nm) is the operating wavelength and p is the scattering size distribution coefficient. According to Kim's model, the values of p are given by equation (14) [3, 8].

$$p = \begin{cases} 1.6 & V\rangle 50 \\ 1.3 & 6\langle V\langle 50 \\ 0.16V + 0.34 & 1\langle V\langle 6 \\ V - 0.5 & 0.5\langle V\langle 1 \\ 0 & V\langle 0.5 \end{cases} \qquad (14)$$

Figure 3 shows the evolution of visibility over time for five selected cities. For the five cities considered, the maximum visibility distance is 10 km and is generally observed during the period from January to the end of March, which is the end of the dry season [20]. The lowest visibility distances are observed during the period from April to August, with a minimum value of 6.55 km observed in Man. The distribution of visibility distances remains the same for all five years. Abidjan has the highest average annual visibility values, with levels generally higher than the national average. Man has the lowest visibility distances, with levels below the national average. During the April to September rainy season, visibility distances in Korhogo, Bouaké and Bondoukou follow the same trend as Man, with values above the national average. Since visibility has a direct influence on the calculation of

Mie scattering, Table 1 shows the maximum, minimum and average visibility ranges and the corresponding Mie scattering coefficients for the five selected cities. In calculating the scattering coefficient, the wavelength of the optical signal is considered as 1550 nm. Table 1 clearly shows that the Mie coefficient depends on visibility distance. The lower the visibility, the higher the Mie coefficient. The city of Man, with the lowest visibility distances, also records the highest Mie coefficient values, with 0.112 dB/km and 0.161 dB/km as minimum and maximum values respectively. This describes the greater atmospheric attenuation in this zone. This can be explained by its mountainous geographical profile and its generally rainy meteorological profile [20]. According to Table 1, the maximum visibility distance in each of the chosen environments is 10 km. Abidjan is the environment with the greatest average visibility distance, at 9.5477 km, with a minimum Mie coefficient of 0.112 dB/km and a maximum coefficient of 0.115 dB/km. The cities of Korhogo, Bouaké and Bondoukou recorded maximum Mie coefficients of 0.132 dB/km, 0.148 dB/km and 0.141 dB/km respectively. This can be explained by the high levels of fog observed in these areas during the harmattan period [21].

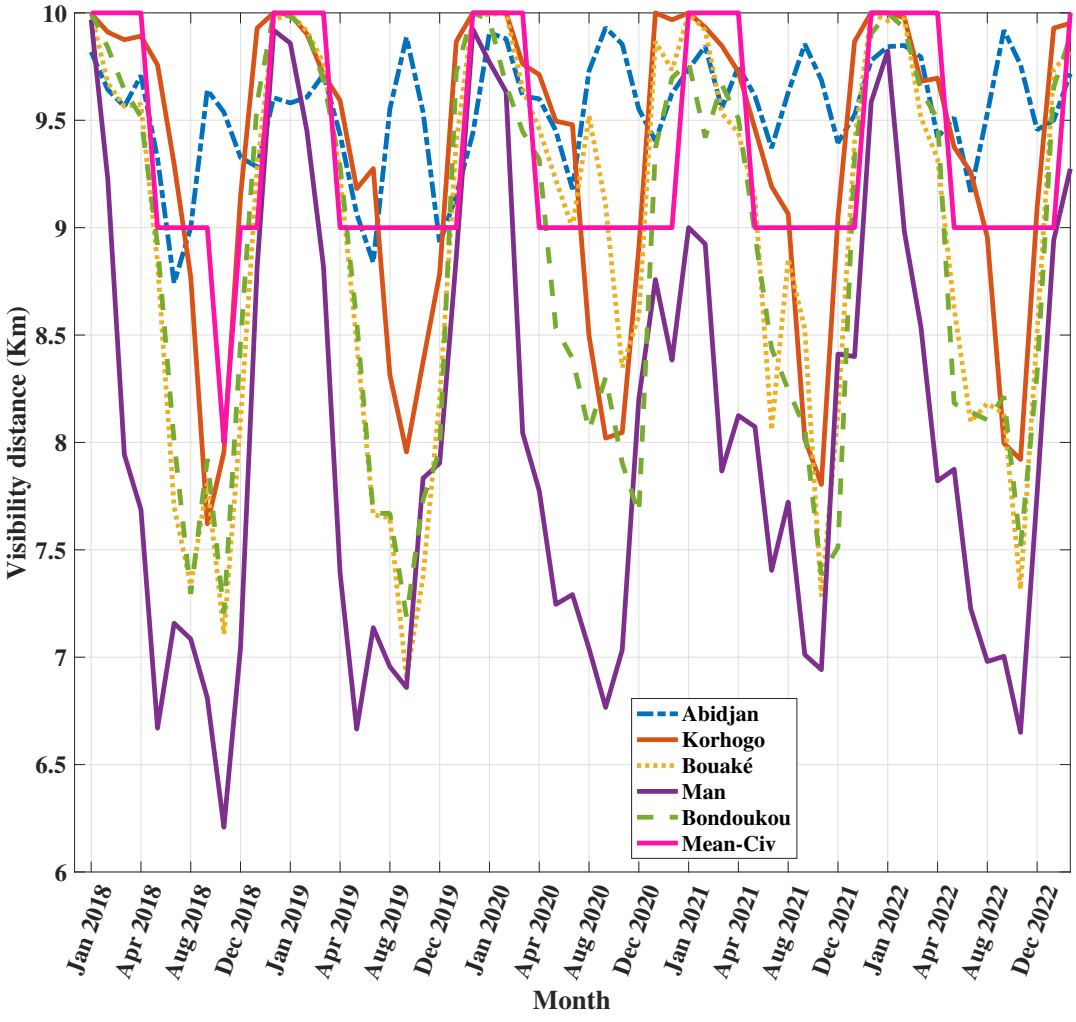

Fig. 3. Visibility distribution per month.

Precipitation is another predominant factor in scattering, it is used to characterize non-selective diffusion, the expression of which is given by equation (15) [1, 5]. Figure 4 shows precipitation levels for the selected cities. The general trend of the precipitation curves is the opposite of that of the visibility curves in our study environments. In general, the rainfall distribution seems to follow the same pattern from one year to the next, with maximum rainfall values between April and October and low values between November and April.

During 2018 and 2019, there was heavy rainfall, with peaks of up to 38 mm/day mainly observed in Man. During 2020, 2021, 2022, there was a general decrease in rainfall with peaks of 17 mm/day observed in Korhogo and Man. Man recorded above-average rainfall levels for almost the whole year. Table 2 summarizes rainfall trends for the five selected cities and also shows rainfall scattering values. The non-selective scattering coefficient changes in proportion to precipitation. The higher the rainfall, the greater the coefficient.

$$\beta_{pluie} = \alpha R^{\rho} \qquad (15)$$

Table 1
Analysis of the Mie diffusion coefficient under Côte d'Ivoire weather conditions.

Cities	Average visibility (km)	Maximum visibility (km)	Minimum visibility (km)	Minimum Mie coefficient (dB/km)	Max Mie coefficient (dB/km)
Abidjan	9.5477	10	8.55	0.112	0.115
Korhogo	9.3129	10	7.52	0.112	0.132
Bouaké	8.9577	10	7	0.112	0.148
Bondoukou	8.8569	10	7.2	0.112	0.141
Man	8.0413	10	6.3	0.112	0.161
Civ	9.3500	10	7.51	0.112	0.132

Table 2
Non-selective scattering due to rainfall under Côte d'Ivoire weather conditions.

Cities	Average rainfall (mm/jour)	Max rainfall (mm/jour)	Min rainfall (mm/jour)	Min Non-Selective coefficient (dB/km)	Max Non-Selective coefficient (dB/km)
Abidjan	5.7434	25	0	0	3.9
Korhogo	5.3375	17	0	0	3.1
Bouaké	4.6316	13	0	0	2.6
Bondoukou	4.4222	13	0	0	2.6
Man	9.7276	38	0	0	5
Civ	6.4333	12	0	0	3

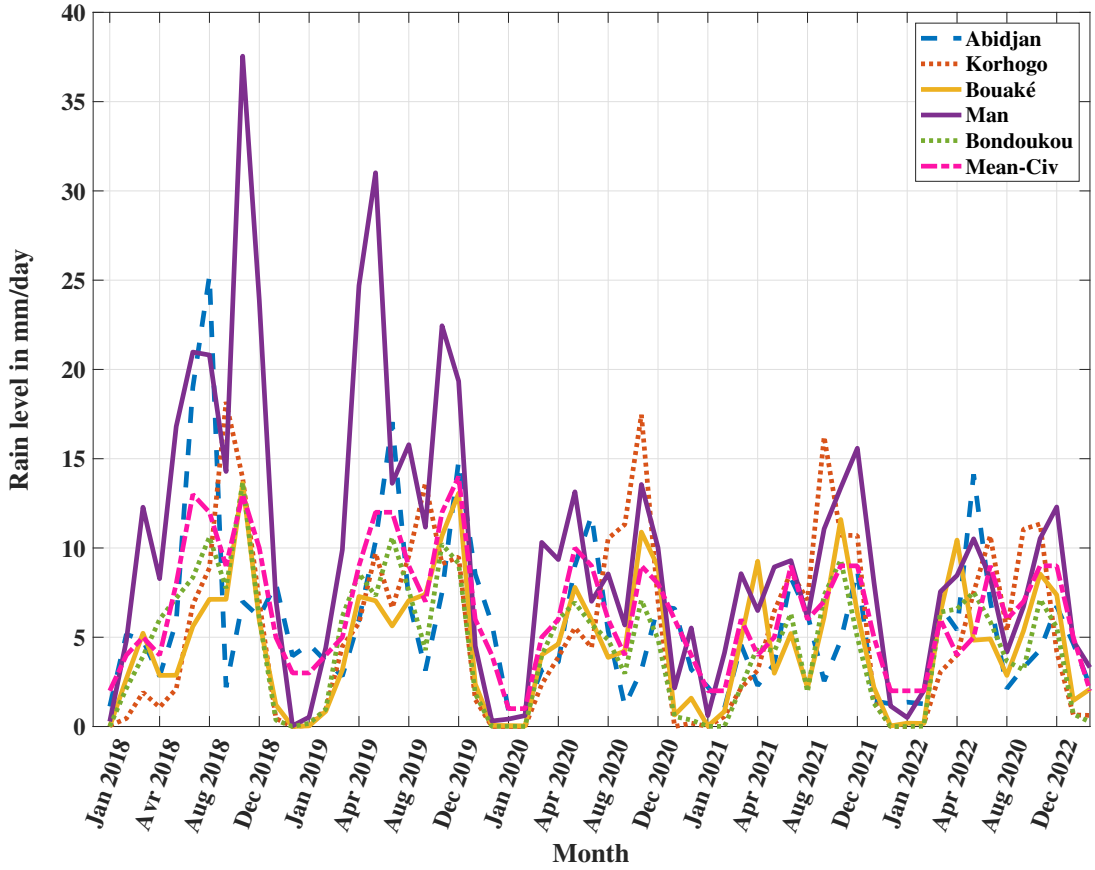

Fig. 4. Rain distribution per month.

Table 2 shows that Abidjan is the second environment where non-selective scattering is most pronounced in Côte d'Ivoire, with an average rainfall value of 5.7434 mm/-day for a maximum non-selective scattering coefficient of 3.9 dB/km. Man environment, where non-selective scattering is highest, records an average precipitation value of 9.7276 mm/day for a maximum non-selective scattering coefficient of 5 dB/km. The non-selective scattering coefficient evolves proportionally to precipitation. The higher the rainfall, the greater the coefficient. The average precipitation in Abidjan, Man, Bouaké and Korhogo is lower than the national average of 6.4333 mm/h. This value is mainly influenced by the high precipitation levels recorded in Man, which counterbalance the relatively low precipitation values observed in the other environments. Table 3 shows the total scattering coefficient for each of our environments. Man, located in the west of Côte d'Ivoire with a sub-equatorial meteorological profile of 5.161 dB/km, has the highest atmospheric scattering level. This is mainly due to the heavy rainfall that occurs there for almost the whole year. The level of diffusion observed in this environment is higher than the national average of 3.132. After Man, the city of Abidjan recorded the highest level of atmospheric diffusion, with a coefficient of 4.015. This is also due to the heavy rainfall observed in this environment, mainly during the rainy season. This rainfall can be explained by the city's proximity to the sea [17]. Korhogo with 3.232 dB/km is the third city in terms of atmospheric diffusion due to rain and visibility. This can be explained by the heavy rainfall observed in this city during the rainy season and by the thick fog encountered during the harmattan

period [21], which contributes greatly to the reduction in visibility distance. The Bondoukou and Bouaké environments are the two with the lowest atmospheric scattering coefficients, 2.741 dB/km and 2.748 dB/km respectively, which is due to the low rainfall observed in these areas. The atmospheric scattering coefficients observed in Korhogo, Bondoukou and Bouaké are lower than the national average of 3.132.

- **Scintillation effect on FSO link**

Scintillation causes the beam to deviate, which considerably degrades the performance of the FSO link and can lead to pointing errors [1,8]. Atmospheric scintillation is the result of variations in the refractive index in the atmosphere. Temperature differences along the optical path lead to a variation in refractive index [7]. The temperature in a given environment below the troposphere changes as a function of wind speed and height [8]. Thus, altitude and wind speed are essential parameters that determine the nature of atmospheric turbulence. The variation in wind speed for the years 2018 to 2022 is shown in Figure 5, based on data collected for the five selected cities. Figure 5 shows that Abidjan has the highest wind speeds, with values ranging from 13 km/h to 22 km/h, with peaks during the rainy season. This is due to the proximity of the city of Abidjan to sea level, which means that it is subject to the full force of the maritime currents. After Abidjan, the towns of Korhogo, Bondoukou and Bouaké have the fastest winds, with speeds ranging from 7.7 km/h to 14.2 km/h, with peaks during the rainy season. This is mainly due to their open plateau-type geography. These speeds follow the variations in wind speed of the national average, which also oscillates between 10 km/h and 14 km/h. Man has the lowest wind speeds, with values ranging from 4.9 km/h to 8 km/h, with peaks during the rainy season. These low values are mainly due to its mountainous geography, which hinders wind movement [22]. For the analysis of atmospheric scintillation levels we consider the gamma-gamma distribution model in each of our environments. This analysis will enable us to classify our environments according to the nature of the turbulence. The parameters to be determined are α (the effective number of small-scale turbulence), β (the effective number of large-scale turbulence), σ^2 (the scintillation index) and C_n^2 (the structure parameter of the refractive index). We always consider the wavelength $\lambda = 1550nm$ and a link distance $L = 10km$. After processing the meteorological data with Matlab, we obtain Table 4, which specifies the parameters of the Gamma-gamma model for each of our environments and the refractive index structure parameter, which is used to assess the strength of atmospheric scintillation for a given environment. The data taken into account for the determination of the parameters are height, wind speed [1,17]. From the data in the Table 4, we can see that the Abidjan environment is one of moderate turbulence, since its structural parameter of the refractive index (C_n^2) is in the order of 10^{-14} [7]. The Korhogo, Bouaké, Man and Bondoukou environments are in the low-turbulence zones with C_n^2 in the order of 10^{-16} [7]. This is due to the height of the environment in relation to sea level, in the Abidjan environment, which is closer to sea level (18 m), variations in the refractive index are greater than in environments such as Korhogo, Man, Bondoukou and Bouaké, which are more than 300 m above sea level. In fact, the closer you get to the ground, the more the atmospheric stratification layers increase [23], which could lead to pointing errors.

- **Error Probability**

The evolution of the probability of error as a function of the signal-to-noise ratio for our two different atmospheric turbulence scenarios is shown in Figure 6. It can be seen from this figure that the curves for the evolution of the probability of error behave in the same way as the curves for the evolution of the signal-to-noise ratio.

Table 3
Total scattering coefficient under Côte d'Ivoire weather conditions.

Cities	Min scattering coefficient (dB/km)	Max scattering coefficient (dB/km)
Abidjan	0.112	4.015
Korhogo	0.112	3.232
Bouaké	0.112	2.748
Bondoukou	0.112	2.741
Man	0.112	5.161
Civ	0.112	3.132

Generally speaking, the probability of error curve for the moderate turbulence environment (Abidjan) and that for the low turbulence environments evolve in opposite ways for signal-to-noise ratio values of less than 5 dB. In fact, we can see that the probability of error curve for Abidjan starts from a maximum value of 0.2 and then decreases towards a probability of error of 0.15. As for the low-turbulence environments (Korhogo, Bouaké, Man and Bondoukou), their error probabilities increase to reach a maximum value of 0.15. From 0.15 the curves follow the same trend and decrease to an error probability of around 0.05 for the Abidjan environment, and around 0.06 for the Korhogo, Bouaké, Bondoukou and Man environments for a signal-to-noise ratio value of 40 dB. Overall, the probability of error is fairly low [1].

3.2 Discussion

Generally in the Ivorian meteorological context, rain is the primary factor causing scattering, resulting in diffusion coefficients of up to 5 dB. This can be explained by the distribution of water droplets, which can be observed through the high levels of daily precipitation. Man recorded the highest scattering coefficients, with a maximum level of 5.161 dB/km. Abidjan and Korhogo recorded maximum atmospheric diffusion coefficients of 3,232 dB/km and 2,748 dB/km. Bouaké and Bondoukou recorded the lowest atmospheric scattering coefficients, with values of 2.748 dB/km and 2.741 dB/km respectively. This is chiefly attributed to the reduced precipitation noted in these regions. The distribution of these coefficients follows the same trend as in Bangladesh, which also has a subtropical climate [5]. Analysis of the probability of error reveals fairly low probabilities, compared with the environment of South Africa where its values can reach 0.9 [24]. Finally, the signal-to-noise ratio values greater than 5 dB demonstrate a threshold value of 0.15, allowing for the prediction of a link availability of 85% in Cote d'Ivoire. The results obtained in this study will make it possible to establish the framework for evaluating the performance of FSO systems for use cases in the field of telecommunications [26]. The characterization of the link helps to evaluate the performance of the FSO system in the Côte d'Ivoire environment. Indeed, although the performance of transmission systems is defined by the technical design of the equipment, knowledge of its propagation environment is essential for estimating the performance of the system, particularly for FSO systems which have

the atmosphere as their propagation channel. Variations in atmospheric turbulence levels can cause FSO performance degradation such as pointing errors, reduction in link capacity, and even link interruption.

Table 4
Atmospheric turbulence parameters for each environment.

	Abidjan	Bouaké	Korhogo	Man	Bondoukou
C_n^2	$1.4466.10^{-14}$	$7.8843.10^{-16}$	$6.7689.10^{-16}$	8.5014^{-16}	$7.2717.10^{-16}$
σ^2	3.8198	0.2082	0.1787	0.2245	0.1920
α	4.2985	11.2662	12.8206	10.5871	12.0591
β	1.3263	9.7428	11.2729	9.0713	10.5243

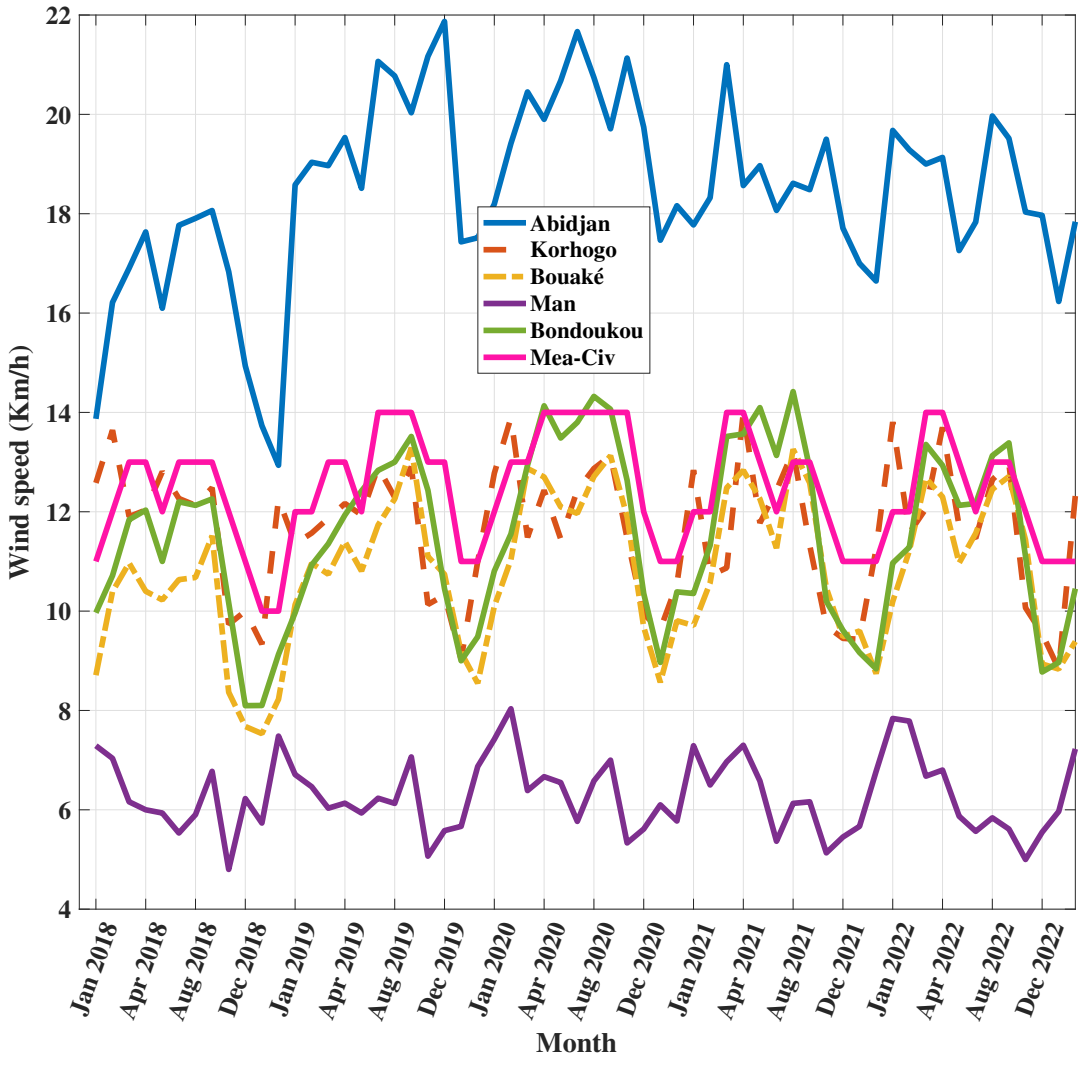

Fig. 5. Wind speed distribution per month.

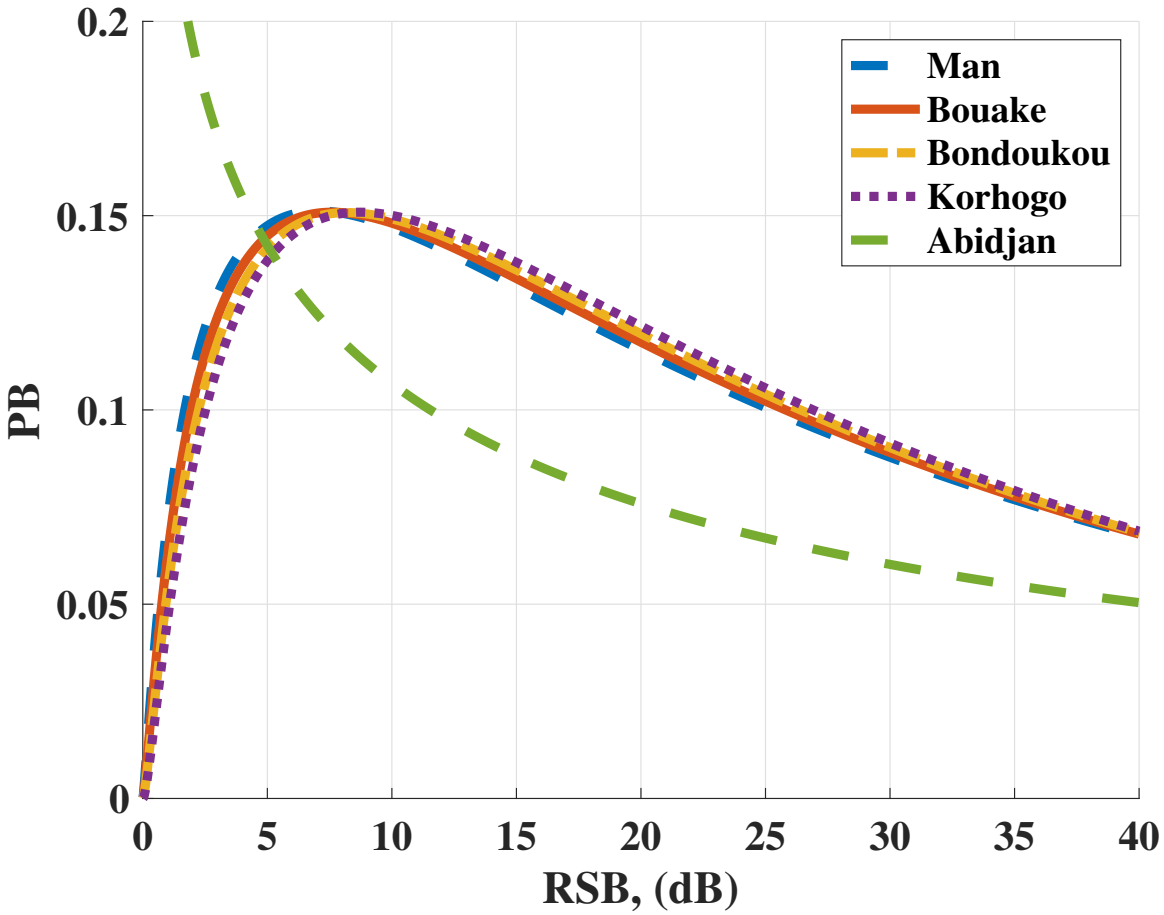

Fig. 6. Error probabilities as function of the signal-to-noise ratio.

The value of availability reveals enormous potential for the development of a mobile network architecture integrating FSO technology as an optimal means of transmission at lower cost.

4 Conclusion

FSO systems operate in the near-infrared optical waveband, a spectral range for which optical components can provide high data rates. The aim of this study was to determine the nature of atmospheric turbulence in Côte d'Ivoire, and to analyze the availability of the FSO link deployed in this environment. Average visibilities, precipitation and wind speed were determined for all sites. Atmospheric scattering and the nature of atmospheric turbulence were modelled using the Gamma-gamma distribution. An assessment of the probability of error was also carried out for our different environments.Signal degradation due to atmospheric conditions was found to be insignificant in the average atmospheric conditions of Côte d'Ivoire. Man is the environment with the highest atmospheric scattering coefficient, at 5.161 dB/km, while Bondoukou and Bouaké have the lowest, at 2.741 dB/km and 2.748 dB/km respectively. Rain is, therefore, the most vital atmospheric scattering factor in Côte d'Ivoire. The results also show that under these average conditions, Abidjan is a moderate-turbulence environment, while Korhogo, Bondoukou, Man and Bouaké are low-turbulence environments. Additionally, the character of atmospheric turbulence is heavily impacted by the altitude of the surroundings. Finally, analysis of the probability of error reveals

that the link can achieve an availability of around 85% in the Côte d'Ivoire environment for SNR values of over 5 dB. Pointing errors are a major hindrance to FSO link operation in certain environments, mainly due to poorly managed atmospheric scintillation [25]. As a follow-up to this study, it may be interesting to analyze the resistance of the link to changes in the factors that can lead to these errors in Côte d'Ivoire.

References

[1] Arun K. Majumdar, *Advanced free space optics (FSO): a systems approach*, Springer 186 (2014).

[2] A. Jahid, M.H. Alsharif, and T.J. Hall, *A contemporary survey on free space optical communication: Potentials, technical challenges, recent advances and research direction*, Journal of Network and Computer Applications 200 (2022) 103311.

[3] P. Sahoo, A. Yadav, *A comprehensive road map of modern communication through free-space optics*, Journal of Optical Communications 0 (2020) 000010151520200238.

[4] S. Derouiche, K. Samir, Haroun E. Adardour, *FSO and MmWave Technologies for 5G Mobile Networks: A Survey*, International Conference on Advances in Electronics, Control and Communication Systems (ICAECCS) IEEE (2023) 1-6.

[5] Kazi Md. shahiduzzaman, Bijoy K. Karmaker, M. Haider, : *Terrestrial Free Space Optical Communications in Bangladesh: Transmission Channel Characterization*, International Journal of Electrical and Computer Engineering (IJECE) 9(4) (2019) 3130-3138.

[6] O.A. Ayo-Akanbi et al. *Impacts of Aerosol Scattering Attenuation on Free-Space Optical Communication in Owerri, Nigeria*, IOP Conference Series: Earth and Environmental Science 1197(1) (2023) 012007.

[7] Ghassemlooy Zabih, Wasiu Popoola, Sujan Rajbhandari, Optical wireless communications: system and channel modelling with Matlab®, CRC press (2019).

[8] L.C. Andrews, and R.L. Phillips, Laser beam propagation through random media. Laser Beam Propagation Through Random Media: Second Edition (2005), ISBN: 9780819478320.

[9] A. Trichili, M.A. Cox, B.S. Ooi, M.S. Alouini, *Roadmap to free space optics*, JOSA B 37(11) (2020) A184-A201.

[10] A. Laourine, A. Stephesse, S. Affes : *Capacity of log normal fading channels*, Proc. of the International Conf. on Wireless Communications and Mobile Computing (IWCMC2007) (2007) 13-17

[11] E. Jakeman, *On the statistics of K-distributed noise*, Journal of Physics A : Mathematical and General 13(1) (1980) 31.

[12] Sirous Tannaz et al., *The effects of negative exponential and k-distribution modeled FSO links on the performance of diffusion adaptive networks,* 9th International Symposium on Telecommunications (IST), IEEE (2018) 19-22.

[13] Dima Bykhovsky, *Simple Generation of Gamma, Gamma-Gamma and K Distributions with Exponential Autocorrelation Function* , Journal of Lightwave Technology 34(9) (2016) 2106 - 2110.

[14] Ehsan Bayaki, Robert Schober, Ranjan K. Mallik, *Performance Analysis of MIMO Free–Space Optical Systems in Gamma–Gamma Fading*, IEEE TRANSACTIONS ON COMMUNICATIONS 57(11) (2009) 3415-3424.

[15] K. Kiasaleh, *Channel estimation for FSO channels subject to Gamma-Gamma turbulence*, Proc. ICSOS (2012) 1-7.

[16] Weather data bank homepage. https://historique-meteo.net

[17] Markus Kottek et al., World map of the Köppen-Geiger climate classification updated (2006).

[18] Z.N. Chaleshtory, A. Gholami, Z. Ghassemlooy, M. Sedghi, *Experimental investigation of environment effects on the FSO link with turbulence*, IEEE Photonics Technology Letters 29(17) (2017) 1435-1438.

[19] Yves K. Kouadio, Delfin A. Ochou, Jacques Servain, *Tropical Atlantic and rainfall variability in Côte d'Ivoire*, Geophysical Research Letters 30(5) (2003).

[20] Gneneyougo Emile Soro, et al. *Estimation des pluies journalières extrêmes supérieures à un seuil en climat tropical: cas de la Côte d'Ivoire*, Physio-Géo. Géographie physique et environnement 10 (2016) 211-227.

[21] G. Canut, Intéraction Mousson/Harmattan, échanges de petite échelle, Doctoral dissertation, Université Paul Sabatier-Toulouse III (2010).

[22] J.M. Wallace, P.V. Hobbs, *Atmospheric science: an introductory survey*, Elsevier 92 (2006)

[23] A.A. Grachev, E.L. Andreas, C.W. Fairall, P.S. Guest, P.O.G. Persson, *The critical Richardson number and limits of applicability of local similarity theory in the stable boundary layer*, Boundary-layer meteorology 147 (2013) 51-82.

[24] O.O. Kolawole, T.J. Afullo, M. Mosalaosi, *Terrestrial free space optical communication systems availability based on meteorological visibility data for South Africa*, SAIEE Africa Research Journal 113(1) (2022) 20-36.

[25] Singh Harjeevan et al., *Design and Analysis of Commercially Viable Free-Space Optical Communication Link for Diverse Beam Divergence Profiles*, Frontiers in Physics 9 (2021) 741.

[26] Brima Abu Bakarr Sahr, Edwin Ataro, and Aladji Kamagate, *Performance enhancement of an FSO link using polarized quasi-diffuse transmitter*, Heliyon 7(11) (2021).